

STRESS PREDICTION ANALYSIS DURING HOT WORKING OF 100MNCrW4 STEEL

Maroš ECKERT

Abstract: This paper deals with the analysis and the possibility of using a constitutive model based on the Arrhenius equation for tool steel 100MnCrW4. Experimental measurements were performed on a DIL 805 dilatometer in the range of strain rate 0.001 s^{-1} for 10 s^{-1} and temperature from 800 to 1200 °C. Using constitutive equations, material parameters and activation energy were derived, which can be subsequently applied to other models related to hot behavior of deformation. The experimental data were compared to the ones obtained by the predictive model with the correlation coefficient $R = 0.97885$ and the parameter $\text{MAPE} = 17.28 \%$ which means a very good level of prediction.

Keywords: Tool steel; Hot working; True stress; Dilatometry; Arrhenius equation.

1 INTRODUCTION

A constitutive equation or model is a mathematical formulation that establishes a quantitative relationship between two parameters, thereby characterizing material properties. Describes how the material responds to external stimuli and loads. These parameters can be stress - deformation, temperature - heat flow, el. voltage - el. current, etc. depending on the dependencies sought [1, 2]. In the case of forming the material at elevated temperatures, there is a dependence between the actual stress and the deformation. At higher temperatures, various metallurgical and structural changes in the material can occur, which the constitutive equation must capture, and thus its complexity increases. At the same time, it is difficult to create a single model that takes into account all the effects of transformation rate, temperature and other metallurgical phenomena on the course of stress.

In material processing, theoretical constitutive models are used to describe the behavior of materials, taking into account the combined effects of strain hardening, hardening due to transformation rate and thermal softening at different rates and transformation temperatures [3,4]. Understanding the behavior of ductile materials is essential for modeling structural changes and processes. This is the basis for a precise solution of the thermo-mechanical behavior of materials using finite element methods. A suitable model must be able to mathematically characterize the mechanical properties and their reactions over a wide range of loads [5]. In constitutive models, most parameters are determined based on experimentally obtained stress profiles, and therefore such models can relatively accurately predict the hot working behavior of a material [6].

This research attempted to represent thermal deformation of 100MnCrW4 tool steel by formulating a proper constitutive correlation. The thermal compression was tested at different temperatures and strain rates. From the obtained data the dependences between stress and deformation were made, the so-called flow curves. The flow stress

was further analyzed based on the test results. A comprehensive constitutive model involving temperature, strain rate, and flow stress was established. Finally, the reliability of the constitutive model was verified.

2 MATERIALS AND METHODS

100MnCrW4 tool steel was used as experimental material. This tool steel is designed for oil hardening with universal use. Alloying elements are manganese, chromium and tungsten. Tools made of this steel have good wear resistance due to the tungsten content, which also contributes to the higher chromium content. Steel shows good hardenability, fine structure and high toughness [7]. Another important feature is the very good dimensional stability after heat treatment. Chemical composition with limit values allowing the relevant standard is given in Tab. 1, basic properties in Tab. 2. The basic microstructure of annealed steel contains fine carbides in a ferritic matrix (Fig. 1) and tempered martensite (dark areas).



Fig. 1 Microstructure of 100MnCrW4 steel
Source: author.

The samples were processed into a dilatometric device in the form of a roller with a diameter of 5 mm and a length of 10 mm. Such samples are inserted horizontally into the working chamber between two ceramic pistons. They are then compressed

at different rates and at different temperatures. The strain rate was set using a dilatometric device and its values were determined based on standard values from practice. In our case, the strain rate was in the range from 0.001 to 10 s⁻¹ and the temperature from 800 to 1200 °C.

3 RESULT AND DISCUSSION

It is based on a phenomenological approach using the Arrhenius equation, transformed into a constitutive equation [8], which expresses the actual stress and strain rate at different temperatures using the Z parameter, known as the Zener-Hollomon parameter [9]. This parameter represents the thermally compensated strain rate, which is widely used to characterize the hot work behavior of materials [10]. This model is based on the assumption that the rate of transformation can be expressed in the form of:

$$\dot{\varphi} = AF(\sigma)\exp\left(-\frac{Q}{RT}\right) \quad (1)$$

where Q is the activation energy of the hot working process and R is the gas constant (R = 8.314 J·mol⁻¹·K⁻¹)

$$F(\sigma) = \begin{cases} \sigma^s & \alpha\sigma < 0.8 \\ \exp(\beta\sigma) & \alpha\sigma > 1.2 \\ [\sinh(\alpha\sigma)]^n & \text{pre v\textsjetky } \sigma \end{cases} \quad (2)$$

where A, s, β, α are material constants. These constants can be determined directly from experimental data obtained from a dilatometric test. These parameters depend on the transformation, so it is necessary to specify them for each strain value. By default, these parameters are determined for true strain values φ from 0.1 to 0.8 in 0.05 increments. The procedure for obtaining the parameters for the individual transformation values is the same, the

following is an example procedure for the values of these parameters for the material 100MnCrW4 and the strain φ = 0.2.

For low stresses, the relationship between the stress and the strain rate is expressed by the power function:

$$\dot{\varphi} = B\sigma^s \quad (\text{for } \alpha\sigma < 0.8) \quad (3)$$

and for high stresses an exponential function:

$$\dot{\varphi} = B'\exp(\beta\sigma) \quad (\text{for } \alpha\sigma > 1.2) \quad (4)$$

where B and B' are material constants independent of the forming temperature. After logarithmization of equations (3) and (4), the equations are obtained:

$$\ln(\sigma) = \frac{1}{s}\ln(\dot{\varphi}) - \frac{1}{s}\ln(B) \quad (5)$$

and

$$\sigma = \frac{1}{\beta}\ln(\dot{\varphi}) - \frac{1}{\beta}\ln(B') \quad (6)$$

Based on equations (5) and (6), it is possible to determine the parameters s as the inverse of the linear regression direction from the graphical dependence ln(σ) vs. ln(φ) as:

$$s = \left[\frac{\partial \ln \dot{\varphi}}{\partial \ln \sigma} \right]_T \quad (7)$$

and the parameter β similar to the inverse of the linear regression direction from the graphical dependence σ vs. ln(φ):

$$\beta = \left[\frac{\partial \ln \dot{\varphi}}{\partial \sigma} \right]_T \quad (8)$$

In Fig. 2a shows the course of the functional dependence according to equation (7) for individual temperature.

Tab. 1 Chemical composition of steel 100MnCrW4 (wt.%)

ISO 4957	C	Mn	Si	Cr	W	V
Min.	0,85	1,80	0,10	0,40	0,40	0,05
Max.	0,95	2,20	0,40	0,65	0,70	0,20
Spectral analysis	0,91	1,83	0,32	0,50	0,64	0,18

Source: author.

Tab. 2 Basic mechanical and physical properties of 100MnCrW4 steel [10]

Mechanical and physical properties	Tensile strength (MPa)	Modulus of elasticity (GPa)	Heat conductivity (W·m ⁻¹ ·K ⁻¹)	Hardness (HV)	Heat capacity (J·kg ⁻¹ ·K ⁻¹)
Value	> 612	193	33	810	465

Source: author.

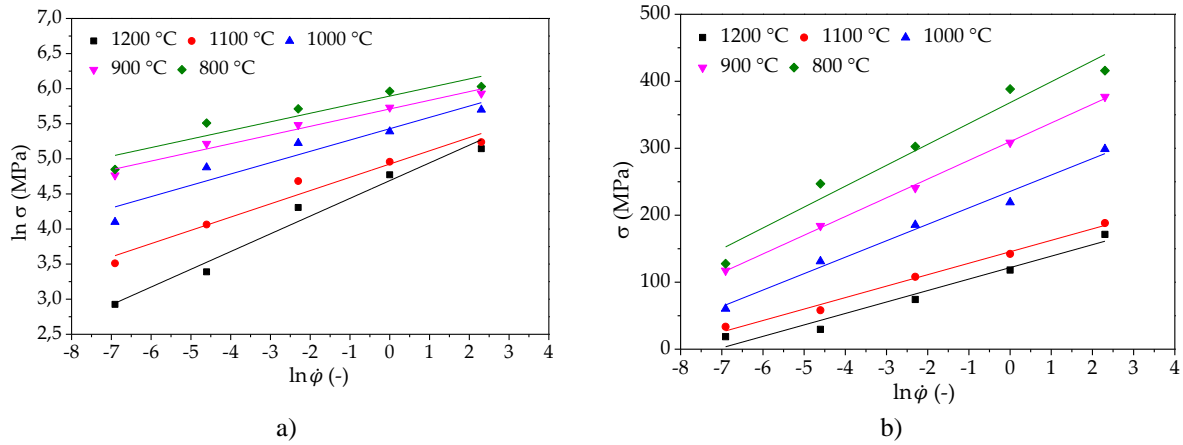


Fig. 2 a) Graphical dependence between $\ln(\sigma)$ vs. $\ln(\dot{\phi})$ to determine the parameter s ; b) graphical dependence between σ and $\ln(\dot{\phi})$ to determine the parameter β
Source: author.

As can be seen, this dependence can be translated by a straight line, and by averaging the inverse value of the directives of the individual straight lines, the value of the parameter s can be obtained. Also in Fig. 2b shows a graphical dependence with the displayed regression lines to determine the parameter β .

For all voltage values (low and high), equation (1) takes the form:

$$\dot{\phi} = A[\sinh(\alpha\sigma)]^n \exp\left(-\frac{Q}{RT}\right) \quad (9)$$

and logarithmizing it to give the form:

$$\ln[\sinh(\alpha\sigma)] = \frac{\ln \dot{\phi}}{n} + \frac{Q}{nRT} - \frac{\ln A}{n} \quad (10)$$

Differentiating equation (10) at constant temperature gives the equation:

$$\frac{1}{n} = \left[\frac{\partial \ln[\sinh(\alpha\sigma)]}{\partial \ln(\dot{\phi})} \right] \quad (11)$$

where the parameter n can again be determined as the inverse average value of the linear regression direction in the graphical dependence between $\ln[\sinh(\alpha\sigma)]$ and $\ln(\dot{\phi})$ for each forming temperature (Fig. 3a).

According to equation (10), it is possible to create a graphical dependence between $\ln[\sinh(\alpha\sigma)]$ and $1000/T$ for each transformation speed (Fig. 3b). The value of the linear regression direction in this case is expressed by the values Q/Rn , from which it is possible to express the values of the activation energy Q . From the intersection of the y-coordinate of the dependence between $\ln[\sinh(\alpha\sigma)]$ and $\ln(\dot{\phi})$ (Fig. 3a) it is possible to determine the parameter $\ln A$ according to the equation:

$$\ln A = \frac{Q}{RT} + \frac{C'}{n} \quad (12)$$

where C' represents the intersection of the y-coordinate by linear regression for each temperature. In this way, the parameters $\ln A$ for the respective temperatures are obtained. Subsequently, using equations (9), it is possible to create a model to determine the stresses depending on the transformation rate and the forming temperature using the determined material parameters such as:

$$\sigma = \frac{1}{\alpha} \left\{ \left[\left(\frac{\dot{\phi} \exp\left(\frac{Q}{RT}\right)}{A} \right)^{\frac{1}{n}} + 1 \right]^{\frac{1}{2}} \right\} \quad (13)$$

In a similar manner, the material parameters are determined for the entire transformation range, which was selected from 0.1 to 0.8 in 0.05 steps. The material parameters depend on the value of the actual deformation and for predicting the voltage in a wide range of temperatures and deformations, the parameters are interpolated by a suitable continuous function. Most often, the obtained parameters are translated by a polynomial function of a certain order [11,12]. The obtained dependences of material parameters were translated by polynomial functions from the 2nd to the 7th degree and the quality of regression was expressed for each degree using the coefficient of determination R^2 . The parameter α show sufficient accuracy of the polynomial regression already at the 3rd degree from which the coefficient of determination did not change

significantly (Fig. 4a). The parameters n , Q and $\ln A$ achieved sufficient regression accuracy at the 5th degree of the polynomial function (Fig. 4b, c, d).

Then the functions describing the material parameters can be expressed by the equations:

$$\alpha = D_0 + D_1\varphi + D_2\varphi^2 + D_3\varphi^3 \quad (14)$$

$$n = E_0 + E_1\varphi + E_2\varphi^2 + E_3\varphi^3 + E_4\varphi^4 + E_5\varphi^5 \quad (15)$$

$$Q = F_0 + F_1\varphi + F_2\varphi^2 + F_3\varphi^3 + F_4\varphi^4 + F_5\varphi^5 \quad (16)$$

$$\ln A = G_0 + G_1\varphi + G_2\varphi^2 + G_3\varphi^3 + G_4\varphi^4 + G_5\varphi^5 \quad (17)$$

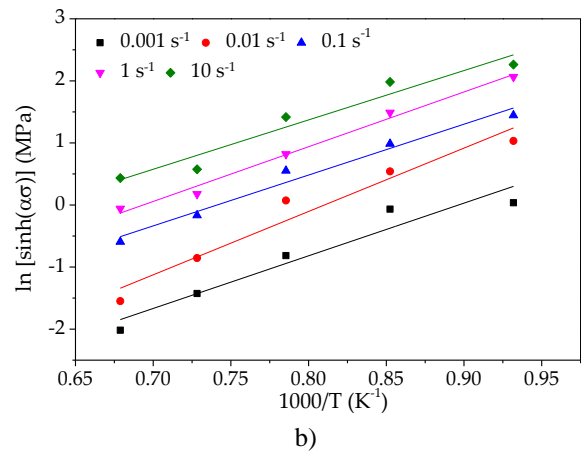
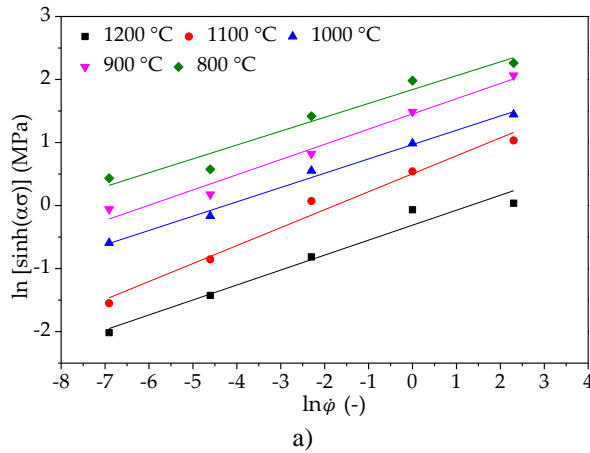


Fig. 3 a) Graphical dependence between $\ln[\sinh(\alpha\sigma)]$ and $\ln(\dot{\varphi})$ to determine the parameter n ; b) graphical dependence between $\ln[\sinh(\alpha\sigma)]$ and $1000/T$ to determine the parameter Q

Source: author.

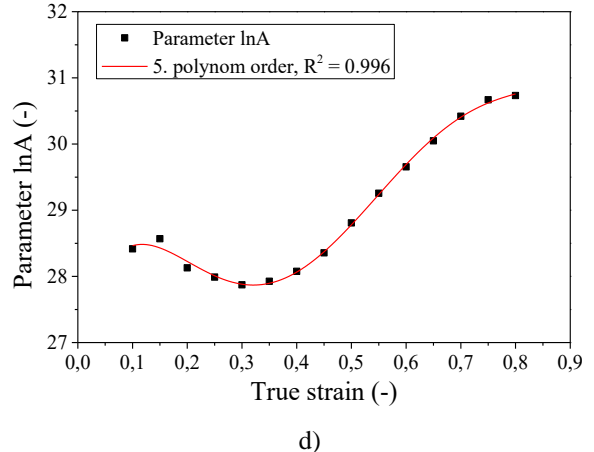
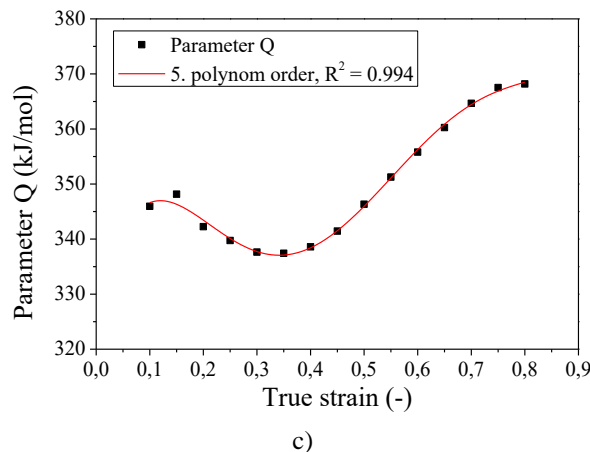
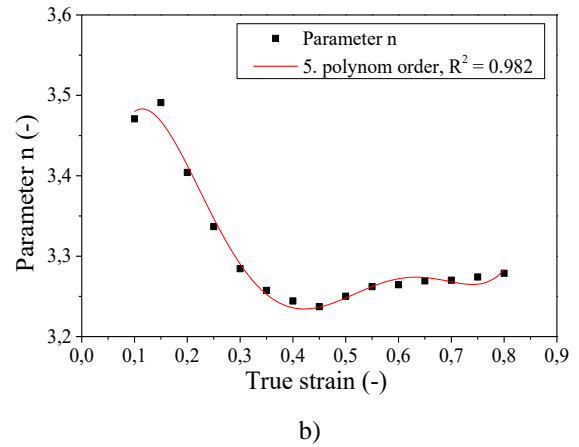
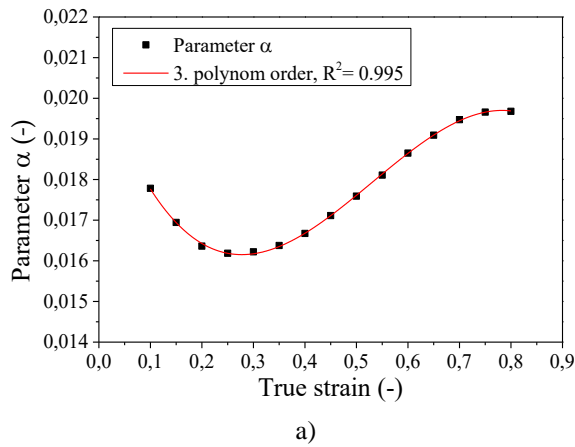


Fig. 4 Course of material parameters for steel X100MnCrW4 depending on deformation: a) parameter α ; b) parameter n ; c) parameter Q ; d) parameter $\ln A$

Source: author.

Tab. 3 Constants of regression polynomial functions of material parameters for steel 100MnCrW4

Parameter α $F_1(\varepsilon)$	Parameter n $F_2(\varepsilon)$	Parameter Q $F_3(\varepsilon)$	Parameter $\ln A$ $F_4(\varepsilon)$
$D_0 = 0,02053$	$E_0 = 3,1745$	$F_0 = 326,1688$	$G_0 = 27,0503$
$D_1 = -0,03577$	$E_1 = 6,5989$	$F_1 = 430,7578$	$G_1 = 30,3846$
$D_2 = 0,08734$	$E_2 = -46,3053$	$F_2 = -2951,4895$	$G_2 = -213,4407$
$D_3 = -0,05492$	$E_3 = 121,8473$	$F_3 = 7668,4699$	$G_3 = 568,5267$
-	$E_4 = -139,2667$	$F_4 = -8241,2172$	$G_4 = -617,4469$
-	$E_5 = 58,3584$	$F_5 = 3161,7272$	$G_5 = 237,4956$

Source: author.

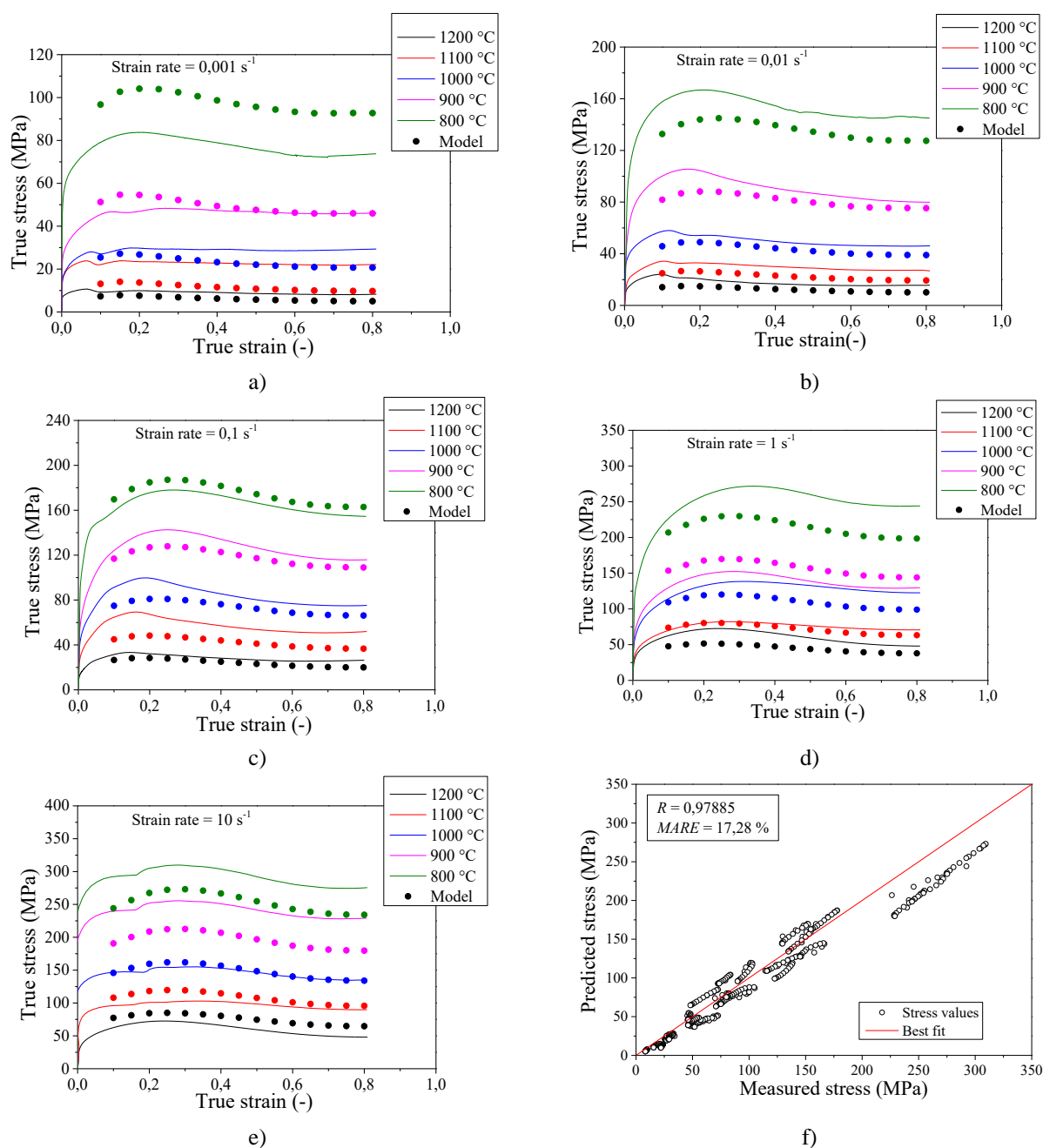


Fig. 5 Comparison between measured and predicted pressure values for 100MnCrW4 material; (a) strain rate $\dot{\varphi} = 0,001 \text{ s}^{-1}$; b) transformation rate $\dot{\varphi} = 0,01 \text{ s}^{-1}$; c) transformation rate $\dot{\varphi} = 0,1 \text{ s}^{-1}$; d) transformation rate $\dot{\varphi} = 1 \text{ s}^{-1}$; e) transformation rate $\dot{\varphi} = 10 \text{ s}^{-1}$; f) correlation between predicted and measured pressure values at all transformation rates with expressed correlation coefficient and MAPE

Source: author.

A comparison of experimental and predicted stress values for 100MnCrW4 material is shown in Fig. 5a-e. The course of stresses was created on the basis of equation (13), into which polynomial functions expressing the development of material parameters depending on the transformation were inserted. The values of the constants of the polynomial functions are given in Tab. 3.

Two statistical parameters were used to assess the overall applicability of a given constitutive model. The first was Pearson's correlation coefficient R and the second was the average absolute percentage error of the forecast ("MAPE"). Both parameters were determined from the stress values at all rates and transformation temperatures. Pearson's correlation coefficient is defined as:

$$R = \frac{E\{[\sigma_E - E(\sigma_E)][\sigma_M - E(\sigma_M)]\}}{\delta_x \delta_y} \quad (18)$$

where E represents the expected value of the actual stress, σ_E and σ_M experimentally and the predicted values of the actual stress, δ_x and δ_y the standard deviations of the stresses. And the MAPE parameter is defined as:

$$MAPE = \frac{1}{n_s} \sum_{i=1}^n \left| \frac{\sigma_E - \sigma_M}{\sigma_E} \right| \cdot 100 \quad (19)$$

where n_s represents the number of all stress values. The quality of the prediction based on the value of the MAPE parameter can be determined on the basis of Tab. 4.

Tab. 4 Prediction quality based on the value of the MAPE parameter [13]

MAPE (%)	Prediction quality
< 10	High
10 – 20	Good
20 - 50	Moderate
> 50	Inaccurate

Source: author.

The values of the predicted stresses are in good agreement with the experiments, which is confirmed by the value of the Pearson's correlation coefficient $R = 0.97885$ and especially the value of $MAPE = 17.28\%$, which can still be considered a good prediction (Fig. 5f). The largest deviations were achieved at the lowest forming temperature of $800\text{ }^\circ\text{C}$, which means that the given temperature forms the limit temperature for the use of this model for the given steel.

4 CONCLUSION

In this work, hot deformation behaviour of 100MnCrW4 steel was investigated at deformation

temperatures from $800\text{ }^\circ\text{C}$ to $1200\text{ }^\circ\text{C}$ and strain rates from 0.001 s^{-1} to 10 s^{-1} . Constructed flow curves were evaluated using a constitutive model based on the Zener-Hollomon parameters.

100MnCrW4 tool steel exhibits DRX (Dynamic Recrystallization) with a single peak stress in the whole range of temperatures and deformation rates. After reaching the peak stresses, it is possible to observe two predominant courses of flow curves. One is a continuous decrease with a significant DRX mechanism, which occurs especially at lower temperatures ($800\text{ }^\circ\text{C} - 1000\text{ }^\circ\text{C}$) or higher strain rates ($1\text{ s}^{-1} - 10\text{ s}^{-1}$) in the entire range of deformation temperatures. The second is only a slight stress drop due to DRX. This course is visible especially at higher temperatures ($1200\text{ }^\circ\text{C} - 1100\text{ }^\circ\text{C}$) and lower strain rates ($0.001\text{ s}^{-1} - 1\text{ s}^{-1}$). This is mainly because under these conditions the higher rate of the DRX slows down the strain hardening. This also shifts the peak and steady stresses to lower values of the true strain. Using a constitutive model based on the Arrhenius equation, it is possible to predict the values of flow stresses in a relatively wide range of temperatures and strain rates. The accuracy of the prediction is at the level of the correlation coefficient $R = 0,97885$ and the parameter $MAPE = 17,28\%$ which means a very good level of prediction.

Acknowledgement

This work was also supported by the Research Agency of the Ministry of Education, Science, Research and Sport of the Slovak Republic under the contract (ITMS2014+) no. 313011W442-CEDITEK II.

References

- [1] BAGHERIPOOR, M. and H. BISADI. Effects of rolling parameters on temperature distribution in the hot rolling of aluminum strips. In: *Applied thermal engineering* [online]. 2011, **31**(10), p. 1556-1565. ISSN 1359-4311. Available at: <http://dx.doi.org/10.1016%2Fj.applthermaleng.2011.01.005>.
- [2] SERAJZADEH, S. and Y. MAHMOOD-KHANI. A combined upper bound and finite element model for prediction of velocity and temperature fields during hot rolling process. In: *International journal of mechanical sciences*. 2008, **50**(9), p. 1423-1431. ISSN 0020-7403. Available at: <https://doi.org/10.1016/j.jimecsci.2008.07.004>
- [3] WANG, X., C. HUANG, B. ZOU, H. LIU, H. ZHU and J. WANG. Dynamic behavior and a modified Johnson-Cook constitutive model of Inconel 718 at high strain rate and elevated temperature. In: *Materials Science & engineering. A Structural materials:*

- properties, microstructure and processing*. 2013, **580**, p. 385-390. ISSN 0921-5093. Available at: <https://doi.org/10.1016/j.msea.2013.05.062>.
- [4] TAN, Q., M. ZHAN, S. LIU, T. HUANG, J. GUO and YANG, H. A modified Johnson–Cook model for tensile flow behaviors of 7050-T7451 alu-minum alloy at high strain rates. In: *Materials science & engineering. A Structural materials: properties, microstructure and processing*. 2015, **631**, p. 214-219. ISSN 0921-5093. Available at: <https://doi.org/10.1016/j.msea.2015.02.010>.
- [5] LAVAKUMAR, A., S. S. SARANGI, V. CHILLA, D. NARSIMHACHARY, and R. K. RAY. A “new” empirical equation to describe the strain hardening behavior of steels and other metallic materials. In: *Materials science & engineering. A Structural materials: properties microstructure and processing*. 2021, **802**, 140641. ISSN 0921-5093. Available at: <https://doi.org/10.1016/j.msea.2020.140641>.
- [6] HUANG, C.Q., H. DENG, J. P. DIAO and X. H. HU. Numerical simulation of aluminum alloy hot rolling using DEFORM-3D. In: *2011 IEEE International Conference on Computer Science and Automation Engineering* [online]. 2011, **3**, pp. 378-381. Available at: <https://doi.org/10.1109/CSAE.2011.5952701>.
- [7] Available at: <https://www.astmsteel.com/product/astm-a1-tool-steel/> [Accessed 8. 3. 2021].
- [8] SAMANTARAY, D., S. MANDAL and A. K. BHADURI. A comparative study on Johnson Cook, modified Zerilli–Armstrong and Arrhenius-type constitutive models to predict elevated temperature flow behaviour in modified 9Cr–1Mo steel. In: *Computational Materials Science*. 2009, **47**, p. 568-576. ISSN 0927-0256. Available at: <https://doi.org/10.1016/j.commatsci.2009.09.025>.
- [9] ZENER, C. and J. H. HOLLomon. Effect of Strain Rate Upon Plastic Flow of Steel. In: *Journal of Applied Physics* [online]. 1944, **15**, p. 22-32. ISSN 1089-7550. Available at: <https://doi.org/10.1063/1.1707363>.
- [10] SHANG, X., Y. CUI and M. W. FU. A ductile fracture model considering stress state and Zener-Hollomon 368 parameter for hot deformation of metallic materials. In: *International journal of mechanical sciences* [online]. 2018, **144**, p. 800-812. ISSN 0020-7403. Available at: <https://doi.org/10.1016/j.ijmecsci.2018.06.030>.
- [11] WEI, G., X. PENG, A. HADADZEDEH, Y. MAHMOODKHANI, W. XIE, Y. YANG and M. A. WELLS. Constitutive modelling of Mg-9Li-3Al-2Sr-2Y at elevated temperatures. In: *Mechanics of materials* [online]. 2015, **89**, p.241-253. ISSN 0167-6636. Available at: <https://doi.org/10.1016/j.mechmat.2015.05.006>
- [12] LI, J., B. GAO, S. TANG, B. LIU, Y. LIU, Y. WANG and J. WANG. High temperature deformation behavior of 380 carbon-containing FeCoCrNiMn high entropy alloy. In: *Journal of alloys and compounds*. 2018, **747**, p. 571-579. ISSN 0925-8388. Available at: <https://doi.org/10.1016/j.jallcom.2018.02.332>.
- [13] MORENO, J.J.M., A. P. POL, A. S. ABAD and BLASCO, B.C. Using the R-MAPE index as a resistant measure of forecast accuracy. In: *Psicothema Revista de Psicologia*. 2013, **25**(4), p. 500-506. ISSN 0214-9915.

Dipl. Eng. Maroš **ECKERT**, PhD.
 Design and Special Technology Department
 Faculty of Special Technology
 Alexander Dubček University of Trenčín
 Ku kyselke 469
 911 06 Trenčín
 Slovak Republic
 E-mail: maros.eckert@tnuni.sk

Maroš Eckert – was born in Ilava, Slovakia in 1989. He received his Master and PhD. degrees at Slovak Technical university, Faculty of Mechanical Engineering in Bratislava. In his research he focuses on materials research, tribology and micro and nanostructural analysis using AFM microscopy.